Nucl. Phys. B 1003 (2024) 116463

Contents lists available at ScienceDirect

Nuclear Physics, Section B

journal homepage: www.elsevier.com/locate/nuclphysb

High Energy Physics – Phenomenology

The XENON program for dark matter direct detection

Elena Aprile

Physics Department, Columbia University, New York, NY 10027, USA

ARTICLE INFO

Editor: Tommy Ohlsson

ABSTRACT

The XENON family of experiments have been at the forefront of direct dark matter searches for weak-scale dark matter for more than fifteen years. In this time, the program has scaled from a few-kilogram pathfinder detector to the current XENONnT holding 8.6 tonne of liquid xenon. Innovations in xenon handling, material selection and purification have allowed each detector generation to feature a lower background rate than the previous.

1. Introduction

The nature of dark matter (DM), the dominant form of matter in the Universe [1], remains unknown despite decades of theoretical and experimental efforts. Its undisputed existence cannot be explained without invoking new physics Beyond the Standard Model (BSM) of particle physics. Weakly Interacting Massive Particles (WIMPs) [2] are compelling DM particle candidates that arise naturally in several BSM theories. WIMPs direct detection via their rare scattering off normal matter in low background experiments has been pursued over the last several decades with a variety of target materials and detector technologies. The best limits on WIMP-nucleon cross section for spin-independent interactions have been achieved by dual-phase Liquid Xenon (LXe) Time Projection Chambers (TPCs) such as the family of detectors operated by the XENON collaboration. This detector technology has led the field for more than fifteen years and continues to be the most promising to cover the remaining expected parameter space, until the dark matter rate becomes comparable with the irreducible background caused by interactions of neutrinos [3]. The Xe high atomic mass number and high liquid density allow for massive yet compact, homogeneous detectors with efficient self-shielding against external radiation. The simultaneous detection of both ionization and scintillation signals down to a few keV enables dual-phase TPCs to reconstruct event positions in 3D, in turn allowing for powerful background suppression via fiducialization of the active liquid target.

These features are exploited by the detectors of the XENON phased program carried out since 2005 at the INFN Laboratori Nazionali del Gran Sasso (LNGS) in Italy, first with the pathfinder XENON10 (14 kg LXe TPC) followed by XENON100 (62 kg LXe), then XENON1T (2.0 t LXe) and the currently operating XENONnT (5.9 t LXe) detector. Results on the WIMP-nucleon scattering cross section achieved by these successive experiments are shown in Fig. 1b. The unprecedented improvement in sensitivity, with a factor of 10 every ∼3.3 years since ∼2007, was only possible thanks to the drastic concomitant reduction in background levels (see Fig. 2), with current lowest electronic background rate in XENONnT of ∼0.3 events/(t d) in the energy region relevant for WIMPs, below 10 keV. In the following we summarize the key features of the different experiments developed within the XENON program and the key results obtained on the search for WIMPs.

E-mail address: ea18@columbia.edu.

https://doi.org/10.1016/j.nuclphysb.2024.116463
Received 9 January 2024; Received in revised form 28 January 2024; Accepted 28 January 2024

Available online 6 May 2024

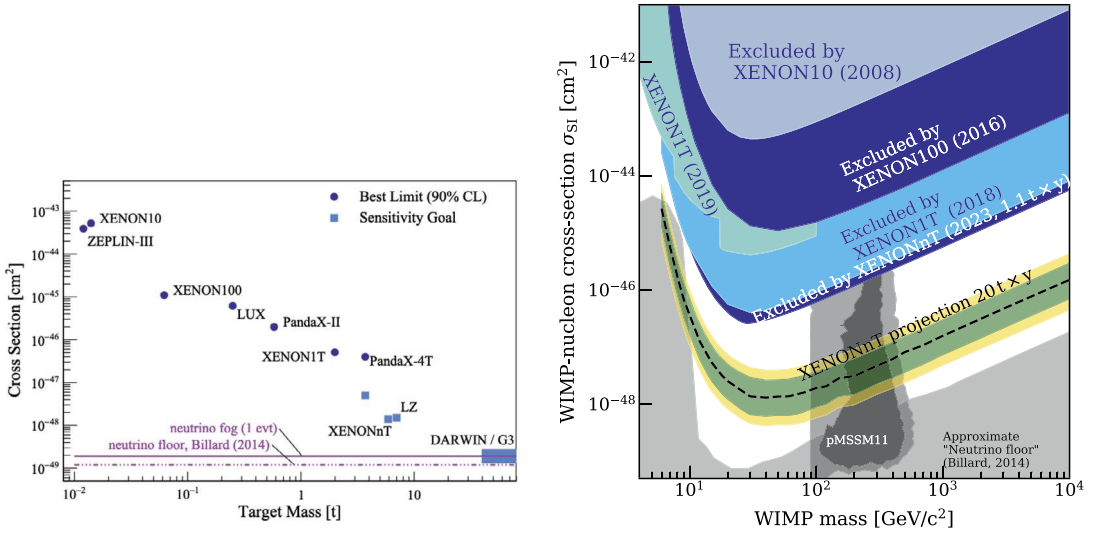

(a) Progress of direct detection limits for LXe TPCs

(b) XENON WIMP-nucleon spin independent cross section constraints

Fig. 1. Progress in WIMP searches with LXe: The plot shows the improvement in sensitivity to spin independent WIMP-nucleon coupling (for a mass of 50 GeV/c^2) achieved by LXe experiments of increasing target masses [4]. The right plot shows successive results from the XENON collaboration [5–9]. The gray region at low cross-sections is one estimate of where the astrophysical neutrino flux will dominate over a dark matter signal, from [10], and the contour shows a supersymmetric parameter scan favored region for WIMP dark matter [11].

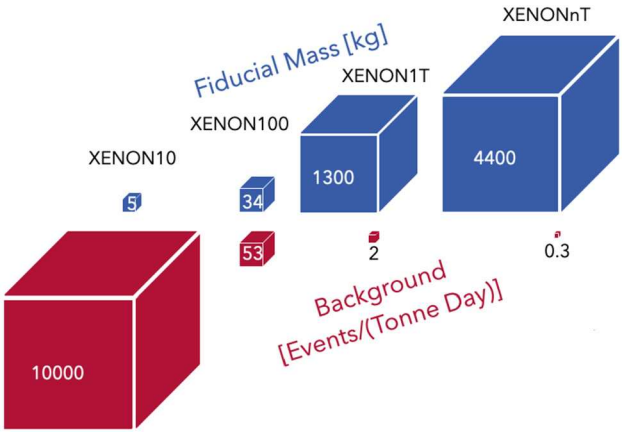

Fig. 2. Evolution of fiducial LXe target mass and electronic recoil background below 10 keV in the XENON detectors, scaled by volume to achieve the required dynamic range.

2. The phases of the XENON program

The detector at the heart of each of the XENON experiments is a dual-phase LXe TPC, in which particle interactions are observed via scintillation and ionization signals, as illustrated in Fig. 3: the first is the prompt scintillation light (S1), while the second is caused by ionization electrons that are drifted and extracted into the gaseous phase where they produce electroluminescence (S2). The photons are detected by two arrays of photomultiplier tubes (PMTs). The difference in arrival time between the S1 and S2 signals yields the depth z of an interaction. The S2 light distribution in the top array yields the (x, y)-position of an event, while the S2/S1 ratio allows discriminating electronic recoils (ERs) from nuclear recoils (NRs), as demonstrated in the XENON10 phase [12], illustrated in Fig. 5c. Fig. 4 lists key characteristics of each XENON experiment.

2.1. XENON10

The first prototype of the XENON family of detectors, XENON10, contained 15 kg of liquid xenon of which 5.4 kg was selected for a WIMPs search [13]. Fig. 5 shows the 1-inch square metal-channel PMTs developed to work in LXe and first used in XENON10, and key results from the XENON10 WIMP search: by operating as a dual-phase TPC, reading out both scintillation light and charge

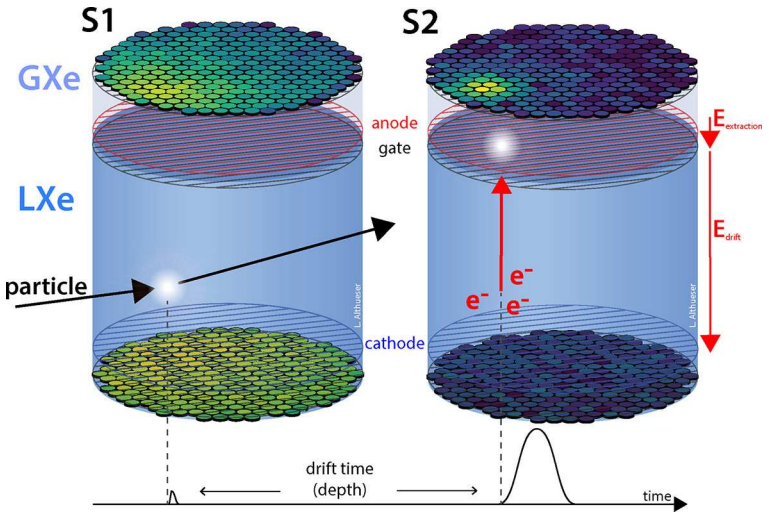

Fig. 3. Principle of operation of a dual phase LXeTPC, courtesy of the XENON collaboration. In the left figure, an incoming particle deposits energy, and the scintillation light is observed in the top and bottom PMT arrays. On the right, ionisation electrons are drifting to the LXe surface, where they will be extracted as an S2 signal carrying position information.

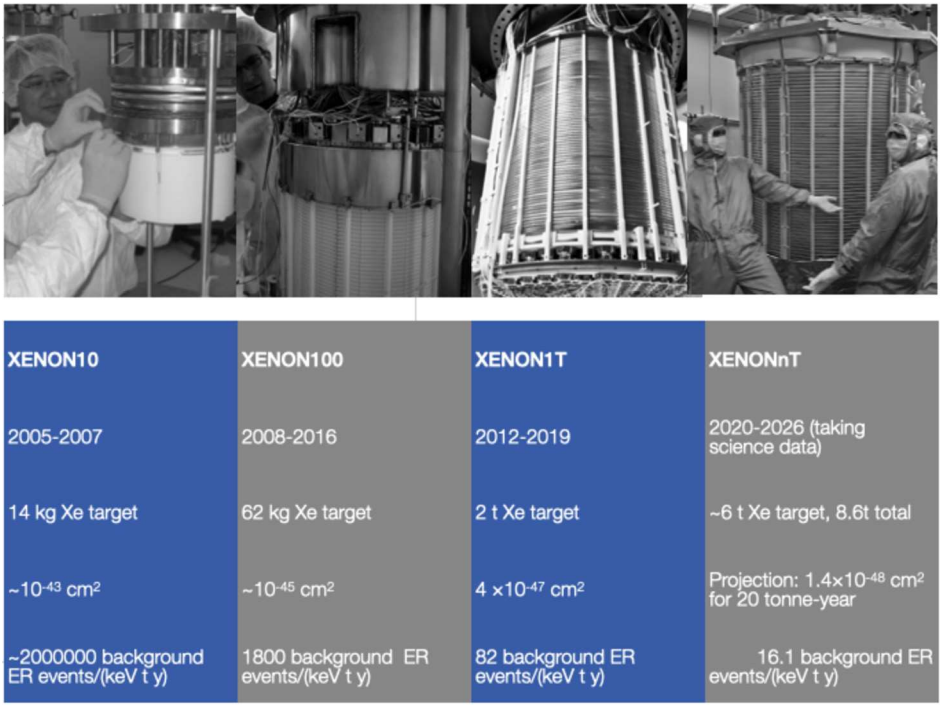

Fig. 4. The experiments of the XENON phased program.

allowed discrimination between electronic and nuclear recoils, as shown in Fig. 5b. The TPC was shielded by a passive polyethylene and lead shield against environmental radiation. The experiment also demonstrated three-dimensional position reconstruction, so that the high-background edges of the xenon target could be excluded from a WIMP search. The resulting science-data, shown in Fig. 5c allowed a striking improvement over then-current limits for WIMPs with masses above 10 GeV/c^2, shown in Fig. 5d. With only a few months of data, XENON10 fully demonstrated the potential of the LXe detector technology, paving the way for the next phases of the XENON program.

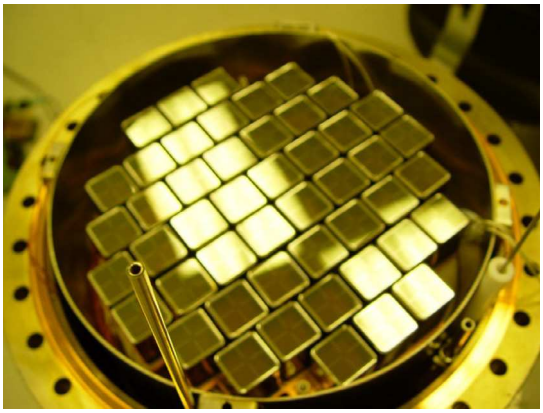

(a) XENON10 PMT array

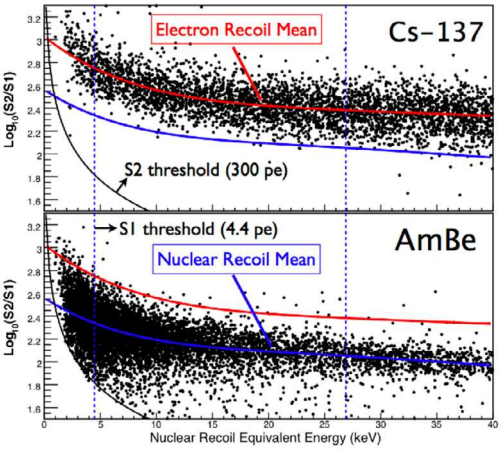

(b) Calibration result from XENON10

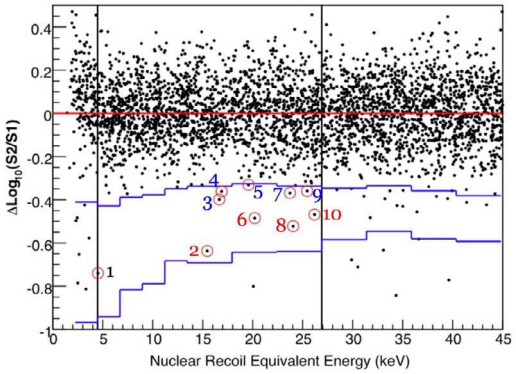

(c) Dark matter search data from XENON10

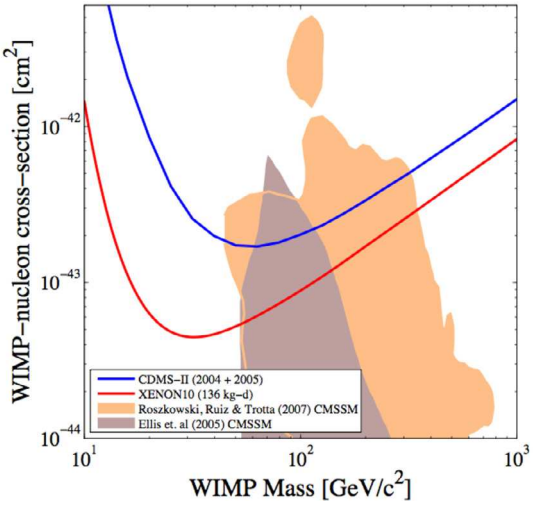

(d) Limits on WIMP-nucleon spin-independent cross-section

Fig. 5. Figures illustrating the XENON10 experiment. Subfigure b) shows the calibration using either a ^{137}Cs ER source, or an AmBe NR calibration source, demonstrating the ER/NR discrimination capability of the technology. Subfigure c) shows the final search data within the search region defined by blue lines [5]. Using a maximum-gap analysis, XENON10 set limits as shown in subfig. d), significantly improving the state-of-the-art.

2.2. XENON100

The XENON100 detector [14] not only scaled up the fiducial mass by almost an order of magnitude, but crucially did so while lowering the background rate by two orders of magnitude [15]. The ∼100 kg mass of LXe surrounding the TPC's volume was instrumented with PMTs to act as an active veto. This feature, in addition to a layer of pure copper close to the TPC's cryostat, improved the shielding against environmental radioactivity with respect to XENON10. In addition, materials used for the XENON100 detector were carefully selected for the lowest intrinsic radioactivity, after an extensive screening campaign. The resulting data in scintillation versus ionization signal is shown in Figs. 6a and 6b. These efforts yielded a significant gain in science reach– nearly two orders of magnitude improvement in the spin-independent WIMP search, as shown in Fig. 6c. Other science channels were also investigated, including a search for axion-like particles [16], leptophilic dark matter [17] and an annual modulation signal [18], among others.

2.3. XENON1T

With XENON1T the collaboration realized the promised scale envisioned in the original XENON proposal to the US National Science Foundation of a tonne-scale detector [19,20], but in one monolithic detector rather than the originally envisioned ten

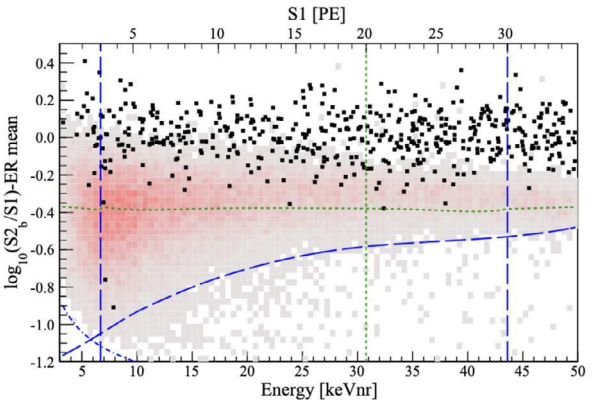

(a) cs1cs2 spectrum

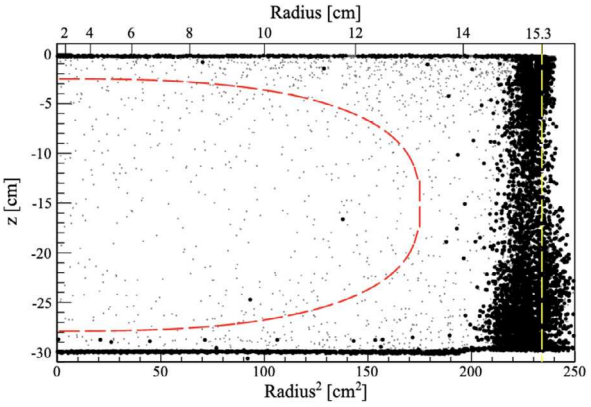

(b) Radius vs Depth

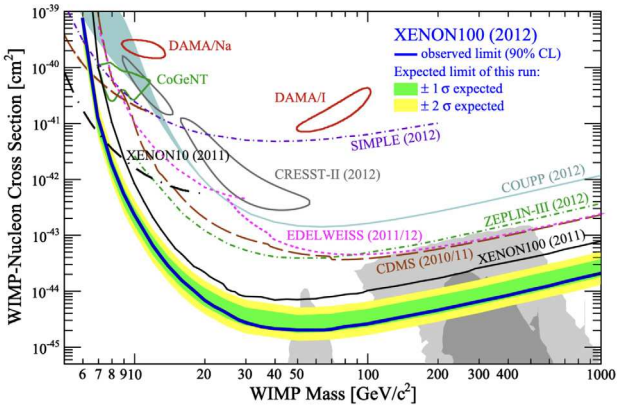

(c) Limits

Fig. 6. Results from XENON100: the scatter plots show the observed events in cS1,cS2 and radius/depth, showing the very good background discrimination in both spaces. The last figure shows the resulting 90% CL upper limits on WIMP-nucleon spin-independent interactions.

identical detectors at the 100-kg scale. The cylindrical TPC measured 96 cm in diameter with a maximum drift length of 97 cm, enclosing a 2 t sensitive volume. Much of the infrastructure built for XENON1T was designed with the vision to rapidly upgrade the experiment with a larger LXeTPC. The 15 m water tank encloses a Cherenkov muon veto detector, to reduce the muon-induced background rate to a negligible level [7], as well as to provide shielding against external backgrounds.

Several new and improved system were developed to handle the challenges associated with the cooling and cleaning of the first tonne-scale LXeTPC, as well as new data acquisition and calibration systems. The XENON1T experiment, located in Hall B of the LNGS, consists of the central LXe detector in its water tank, flanked by a three-story service building shown in Fig. 7a, dwarfing the XENON100 setup which was contained in an office-sized niche at LNGS. The LXe volume, including both the instrumented volume and that contained in non-instrumented regions, totaled 3.2 t, continuously cooled and purified by the cryogenics infrastructure. A spherical storage and recovery sphere was designed to safely contain the entire xenon mass to be recovered from the detector in case of an emergency, and for the xenon to be liquefied and purified before filling the detector. After filling the detector, the xenon is continuously circulated through rare-gas purifiers to remove electronegative impurities that absorb drifting electrons and therefore reduce the S2 signal. The xenon flow can also be routed to a cryogenic krypton distillation column, to remove krypton, including the radioactive ^{85}Kr background source. XENON1T demonstrated the *online* removal of krypton, achieving a reduction in the ^{nat}Kr/Xe ratio from 60 ppb to 0.36 ± 0.06 ppt after 70 days of distillation [21]. The reduction is shown in Fig. 8a.

The primary science results from XENON1T used a total of 278.8 d of exposure from November 2016 until February 2018, divided in two science runs. The analysis of both science runs was performed blinded to reduce experimenter bias, and yielded strong constraints on spin-independent WIMP-nucleon interactions. The WIMP constraints from the analysis of the full exposure, which used an analysis volume containing 1.3 t, for a 1.0 t y exposure, are shown in Fig. 1b. This figure also includes constraints from XENON1T using only the scintillation signal, in order to lower the energy threshold [8], providing results comparable or better than dedicated low-threshold detectors.

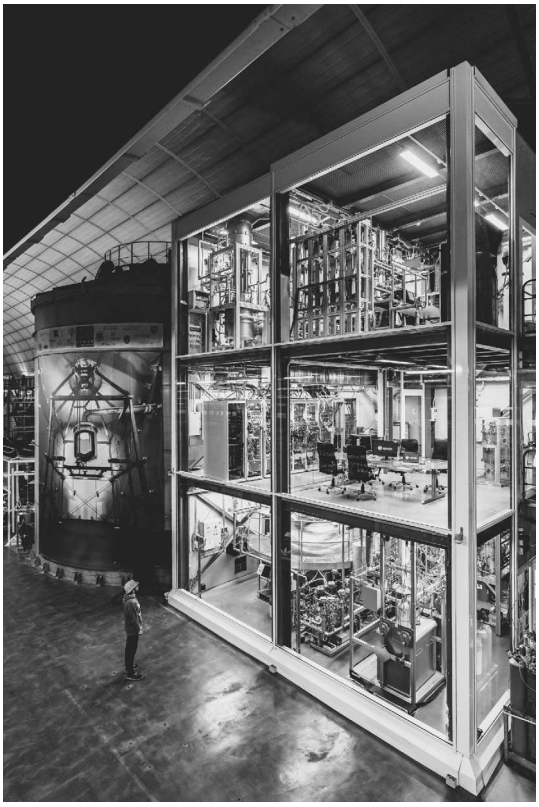

(a) The XENON1T set-up in the LNGS Hall B

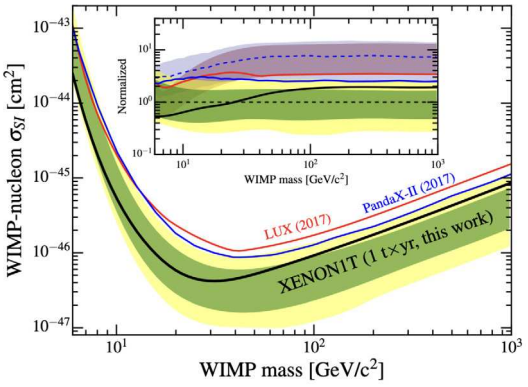

(b) 90 percent confidence limits on spin-independent WIMP-nuclear interactions from XENON1T (black) [7]. Yellow and green bands indicate the 1- and 2-sigma expected fluctuations of the upper limit. The inset shows the ratio between the sensitivity and the final upper limit, illustrating the significant variability of rare event searches.

Fig. 7. XENON1T infrastructure and results.

2.4. XENONnT

Using the same water shield, and much of the infrastructure developed and tested with XENON1T, the upgraded XENONnT phase, started science data-taking in 2021, with a 97.1 d first exposure. The new and larger TPC measures 1.33 m in diameter, and 1.49 m in height, and features twice as many PMTs as XENON1T, 494 in total. It is enclosed in a vacuum insulated vessel containing a total 8.3 tonne of LXe of which 5.9 tonne make the active WIMP target. Of these 4.4 t were chosen for the first science analysis [22].

Surrounding the TPC is a new active neutron veto, which consists of an optically separated and instrumented core of the muon veto water tank with 120 PMTs and a projected neutron tagging efficiency of 0.87 when the water is doped with Gd.

XENONnT also features significant advances in xenon purification. The electron lifetime achieved is an unprecedented >10 ms thanks to an innovative liquid purification technology that can process the entire xenon volume of 8.3 tonne in 18 hours [23]. At low recoil energies relevant for both searches for electronic recoil and WIMP signatures < 20 keV, the background is dominated by single-beta decays of the ^{222}Rn-daughter ^{214}Pb [22]. XENONnT uses a new Rn distillation system capable of operating with high flow, 91 ± 2 kg/h, of xenon [24]. Fig. 8b shows the performance of the column, both in a gas-only mode used for the first science run, reaching 1.8μBq/kr, and the full-flow mode where a further factor 2 reduction was achieved.

The first science run of XENONnT (SR0) was dedicated to probe the nature of an intriguing excess observed in XENON1T: a peak in the spectrum of electronic recoil events compatible with a 2.3 keV peak from solar axions or from a new background, such a very small contamination of tritiated hydrogen molecules [25]. The analysis blinding strategy was adapted to also cover signals in the electronic recoil band, and dedicated side-band runs were collected where a tritium signal, if any, would be amplified by by-passing purification systems. Fig. 9 shows the blinding regions for both the ER and NR searches, together with representative signals for each. The resulting analysis of 1.16 t y featured the lowest ever background rate achieved in a dark matter detector, 16.1 ± 1.3 events/(tonne × year × keV), and found no excess, as shown in Fig. 10a. This conclusively ruled out any new physics explanation of the XENON1T excess, placing strong limits, as shown in Fig. 10b.

XENONnT also performed a search for WIMPs with the same dataset. The data, shown in Fig. 10, had no significant excess with respect to the background model ($p > 0.2$), but limits reflect this $+1\sigma$ fluctuation, and are shown in Fig. 1b. For WIMP searches, two-phase LXe TPCs benefit from a significant discrimination between the nuclear recoil signal events and the more numerous electronic recoil background. The XENONnT response to neutrons was calibrated using an external AmBe source whereas for the response to electronic recoils, internal calibration sources were used. The first science run used ^{83m}Kr data to characterize the detector spatial

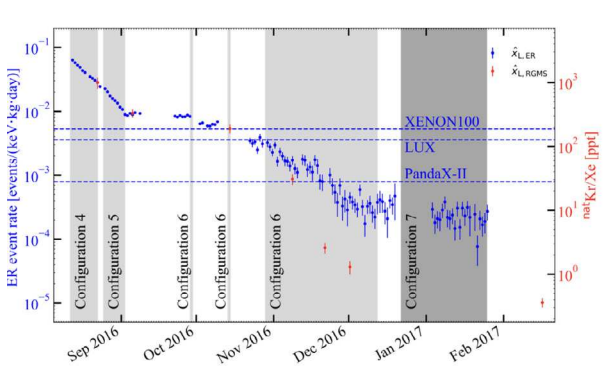

(a) Reduction in krypton concentration in XENON1T due to the Kr distillation column.

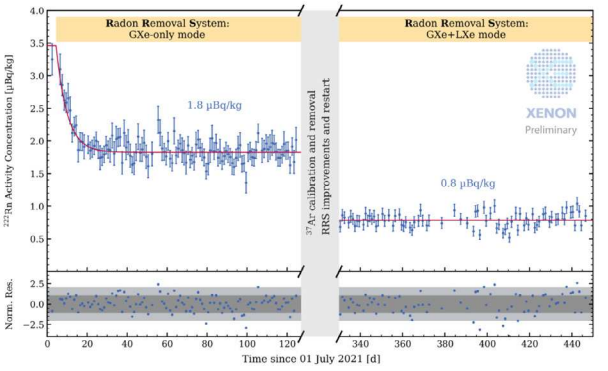

(b) XENONnT level of ^{222}Rn as funciton of time, showing the reduction achieved with the radon column operated both in gas-only and full-flow mode

Fig. 8. Online removal of intrinsic radioactive sources by cryogenic distillation. XENONnT has achieved the lowest intrinsic background level of a LXe TPC to-date.

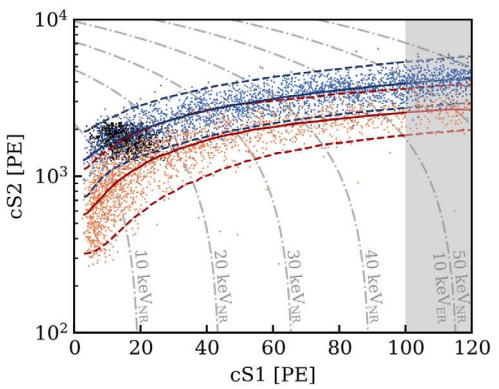

(a) Low-energy calibrations of the XENONnT SR0 analysis: black dots show the 2.8 keV ^{37}Ar calibration line, blue ^{220}Rn beta ER calibration events, and orange the AmBe NR calibration, whose spectrum resembles a 50 GeV/c^2 WIMP

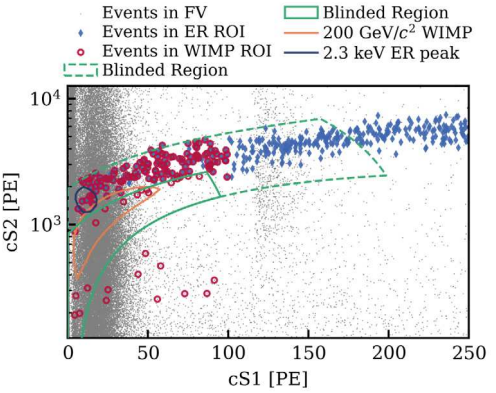

(b) Blinding procedure in XENONnT:gray dots show all events, blue and red dots show events passing the ER and NR search criteria, respectively. Contours show two signals of interest: a low-energy ER peak similar to the one found in XENON1T, and a WIMP spectrum. The dashed green line surrounds the region blinded for the ER search, while the full line surrounds the region blinded for the WIMP search.

Fig. 9. Calibration data and unblinded search data from the XENONnT SR0 [9].

response, correcting for geometric light collection efficiency, electrode sagging and other effects. ^{220}Rn calibration data provided a low-energy approximately flat spectrum of beta-induced ERs, while ^{37}Ar provided a 2.8 keV K-shell decay after an electron capture. Both these sources were fitted with a fast detector simulation model [9] which provided a good fit to the data. Fig. 9 shows the lowest-energy calibration data collected for XENONnT, and illustrates the power of the LXeTPC to distinguish the more common ER background and a NR signal, represented with blue and red contour lines, respectively, for the radon calibration and AmBe data.

Following its first science run, XENONnT is collecting further data, with the reduction of Rn from both gas and liquid Xe and with the neutron veto operating with Gd doping. Similar to the XENON1T efforts, the collaboration is also working to realize the full range of science potential by investigating other signatures, such as low-threshold ionization-only searches, lowering the NR S1 coincidence threshold, and using the ultra-low ER background to improve on searches for high-energy ER signatures, among others.

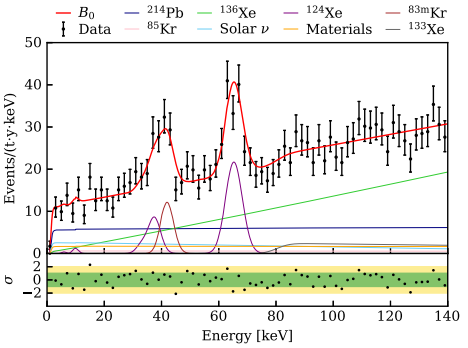

(a) The SR0 ER data set showing background contributions between 0 and 140 keV [22].

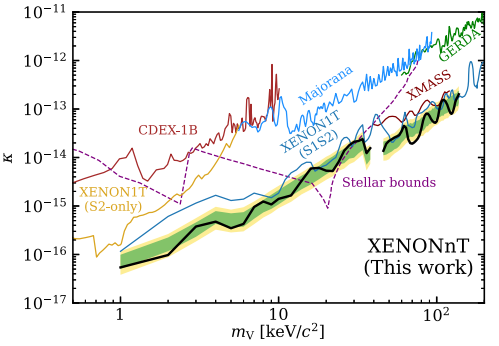

(b) Upper limits on dark photon interactions from the XENONnT ER search [22]

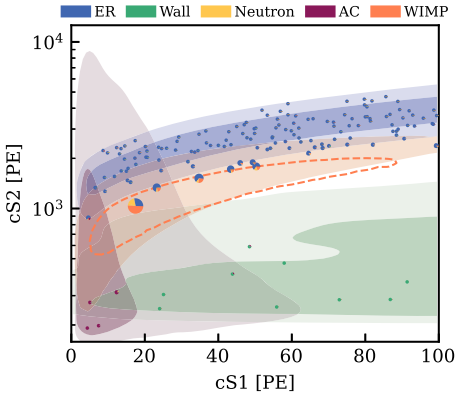

(c) The SR0 WIMP search data set, and contours showing the background 1,2-σ contours. The dashed orange contour shows the most signal-like region [9]

Fig. 10. Results from the XENONnT experiment: data and an example upper limit from the ER search, and the NR search data.

3. Summary

The XENON dark matter program has successfully demonstrated the application of the LXeTPC detector technology as one of the most promising for WIMP direct detection, with a series of experiments which have led the field for almost two decades. The target mass scalability from the few kg-scale to the multi-tonne-scale was accompanied by an unprecedented five orders of magnitude reduction of the intrinsic background, thanks to careful xenon handling, material screening and selection, LXe purification and cryogenic distillation for the reduction of intrinsic radioactivities. The progress in WIMP limits is shown in Fig. 1b, and is now being accompanied by an increasing menu of other new physics or rare events searches.

Declaration of competing interest

The authors declare that they have no known competing financial interests or personal relationships that could have appeared to influence the work reported in this paper.

Data availability

No data was used for the research described in the article.

References

[1] N. Aghanim, et al., Planck 2018 results. VI. Cosmological parameters, Astron. Astrophys. 641 (2020), https://doi.org/10.1051/0004-6361/201833910, Astron. Astrophys. 652 (C4) (2021) A6, arXiv:1807.06209 [astro-ph.CO].

[2] Leszek Roszkowski, Enrico Maria Sessolo, Sebastian Trojanowski, WIMP dark matter candidates and searches – current status and future prospects, Rep. Prog. Phys. 81 (6) (2018) 066201, https://doi.org/10.1088/1361-6633/aab913, arXiv:1707.06277 [hep-ph].
[3] Ciaran A.J. O'Hare, New definition of the neutrino floor for direct dark matter searches, Phys. Rev. Lett. 127 (25) (2021) 251802, https://doi.org/10.1103/PhysRevLett.127.251802, arXiv:2109.03116 [hep-ph].
[4] D.S. Akerib, et al., Snowmass2021 cosmic frontier dark matter direct detection to the neutrino fog, Snowmass 2021 (2022), arXiv:2203.08084 [hep-ex].
[5] J. Angle, et al., First results from the XENON10 dark matter experiment at the gran sasso national laboratory, Phys. Rev. Lett. 100 (2008) 021303, https://doi.org/10.1103/PhysRevLett.100.021303, arXiv:0706.0039 [astro-ph].
[6] E. Aprile, et al., XENON100 dark matter results from a combination of 477 live days, Phys. Rev. D 94 (12) (2016) 122001, https://doi.org/10.1103/PhysRevD.94.122001, arXiv:1609.06154 [astro-ph.CO].
[7] E. Aprile, et al., Dark matter search results from a one ton-year exposure of XENON1T, Phys. Rev. Lett. 121 (11) (2018) 111302, https://doi.org/10.1103/PhysRevLett.121.111302, arXiv:1805.12562 [astro-ph.CO].
[8] E. Aprile, et al., Light dark matter search with ionization signals in XENON1T, Phys. Rev. Lett. 123 (25) (2019) 251801, https://doi.org/10.1103/PhysRevLett.123.251801, arXiv:1907.11485 [hep-ex].
[9] E. Aprile, et al., First dark matter search with nuclear recoils from the XENONnT experiment, Phys. Rev. Lett. 131 (4) (2023) 041003, https://doi.org/10.1103/PhysRevLett.131.041003, arXiv:2303.14729 [hep-ex].
[10] J. Billard, L. Strigari, E. Figueroa-Feliciano, Implication of neutrino backgrounds on the reach of next generation dark matter direct detection experiments, Phys. Rev. D 89 (2) (2014) 023524, https://doi.org/10.1103/PhysRevD.89.023524, arXiv:1307.5458 [hep-ph].
[11] E. Bagnaschi, et al., Likelihood analysis of the pMSSM11 in light of LHC 13-TeV data, Eur. Phys. J. C 78 (3) (2018) 256, https://doi.org/10.1140/epjc/s10052-018-5697-0, arXiv:1710.11091 [hep-ph].
[12] E. Aprile, et al., Simultaneous measurement of ionization and scintillation from nuclear recoils in liquid xenon as target for a dark matter experiment, Phys. Rev. Lett. 97 (2006) 081302, https://doi.org/10.1103/PhysRevLett.97.081302, arXiv:astro-ph/0601552.
[13] E. Aprile, et al., Design and performance of the XENON10 dark matter experiment, Astropart. Phys. 34 (2011) 679–698, https://doi.org/10.1016/j.astropartphys.2011.01.006, arXiv:1001.2834 [astro-ph.IM].
[14] E. Aprile, et al., The XENON100 dark matter experiment, Astropart. Phys. 35 (2012) 573–590, https://doi.org/10.1016/j.astropartphys.2012.01.003, arXiv:1107.2155 [astro-ph.IM].
[15] E. Aprile, et al., Dark matter results from 225 live days of XENON100 data, Phys. Rev. Lett. 109 (2012) 181301, https://doi.org/10.1103/PhysRevLett.109.181301, arXiv:1207.5988 [astro-ph.CO].
[16] E. Aprile, et al., First axion results from the XENON100 experiment, Phys. Rev. D 90 (6) (2014), https://doi.org/10.1103/PhysRevD.90.062009, Erratum: Phys. Rev. D 95 (029904) (2017) 062009, arXiv:1404.1455 [astro-ph.CO].
[17] E. Aprile, et al., Exclusion of leptophilic dark matter models using XENON100 electronic recoil data, Science 349 (6250) (2015) 851–854, https://doi.org/10.1126/science.aab2069, arXiv:1507.07747 [astro-ph.CO].
[18] E. Aprile, et al., Search for event rate modulation in XENON100 electronic recoil data, Phys. Rev. Lett. 115 (9) (2015) 091302, https://doi.org/10.1103/PhysRevLett.115.091302, arXiv:1507.07748 [astro-ph.CO].
[19] E. Aprile, et al., The XENON dark matter search experiment, in: F. Avignone, W. Haxton (Eds.), Nucl. Phys. B, Proc. Suppl. 138 (2005) 156–159, https://doi.org/10.1016/j.nuclphysbps.2004.11.036, arXiv:astro-ph/0407575.
[20] E. Aprile, et al., The XENON1T dark matter experiment, Eur. Phys. J. C 77 (12) (2017) 881, https://doi.org/10.1140/epjc/s10052-017-5326-3, arXiv:1708.07051 [astro-ph.IM].
[21] E. Aprile, et al., First dark matter search results from the XENON1T experiment, Phys. Rev. Lett. 119 (18) (2017) 181301, https://doi.org/10.1103/physrevlett.119.181301, arXiv:1705.06655 [astro-ph.CO].
[22] E. Aprile, et al., Search for new physics in electronic recoil data from XENONnT, Phys. Rev. Lett. 129 (16) (2022) 161805, https://doi.org/10.1103/PhysRevLett.129.161805, arXiv:2207.11330 [hep-ex].
[23] G. Plante, et al., Liquid-phase purification for multi-tonne xenon detectors, Eur. Phys. J. C 82 (10) (2022) 860, https://doi.org/10.1140/epjc/s10052-022-10832-w, arXiv:2205.07336 [physics.ins-det].
[24] M. Murra, et al., Design, construction and commissioning of a high-flow Radon removal system for XENONnT, Eur. Phys. J. C 82 (12) (2022), https://doi.org/10.1140/epjc/s10052-022-11001-9, arXiv:2205.11492 [physics.ins-det].
[25] E. Aprile, et al., Excess electronic recoil events in XENON1T, Phys. Rev. D 102 (7) (2020) 072004, https://doi.org/10.1103/PhysRevD.102.072004, arXiv:2006.09721 [hep-ex].